Chapter 3
Rate-Acceleration of a Light-Driven Rotary Molecular Motor: Fluorenyl-Based Systems

The rotary speed of fluorenyl-based second-generation molecular motors is well tunable, as subtle structural variations have a dramatic influence on the Gibbs energy barrier to the rate determining thermal helix inversion steps. By replacing the naphthalene moiety present in the upper-half in the original design by a sterically less demanding methoxy-substituted phenyl group, the fastest artificial light-driven rotary molecular motor developed so far is obtained, which is in principle capable of operating at 3325 revolutions per second.[*]

[*] Parts of this chapter will be submitted for publication: A. Cnossen, D. Pijper, T. Kudernáč, M. M. Pollard, B. L. Feringa, manuscript in preparation.

3.1 Introduction

In the previous chapter, the initial attempts to increase the rate of rotation of the light-driven unidirectional molecular motors based on sterically overcrowded alkenes were described. The change in design to the second-generation molecular motors was shown to greatly facilitate the analysis of the effects of structural variations.[1] The work described in the previous chapter eventually established a system that can operate with a half-life for thermal isomerization at room temperature of 40 sec, which allows for full rotation at 20°C at the scale of minutes instead of hours.[2] This system however still can hardly compete with Nature's prototypical rotary motor, ATPase, which is capable of transforming the energy of the hydrolysis of approximately 390 molecules of ATP per second into rotational motion at a rate of 130 revolutions per second.[3] To create a system that can rotate at a similar rate, somehow the energy barrier for the rate determining thermal isomerization step needs to be lowered even further.[4] Although electronic factors appeared to also have some influence on the energy barrier to this thermal isomerization,[2] steric effects still seem to dominate in determining its magnitude.[4]

Steric factors seem to have a particularly pronounced effect in the case of the fluorenyl based second-generation molecular motors, which will first be introduced in this chapter. Subsequently, a change in molecular architecture will be presented, which replaces the naphthalene group in the upper-half by a methoxy substituted phenyl moiety, that results in a dramatic increase of the motor's rotation speed.

3.2 Second-Generation Molecular Motors Containing a Five-Membered Ring in the Upper-Half

As described in the previous chapter, decreasing the size of the bridging atom X in the upper-half six-membered heterocyclic ring has a large effect in decreasing the energy barrier for the thermal helix inversion (see Chapter 2, Table 2.1). To take this principle one step further, the bridging atom was completely eliminated: a design change that was already applied on the first-generation motors where it had a pronounced effect on the thermal isomerization barrier.[5] A series of second-generation motors with various lower-halves, all containing a fused five-membered ring in the upper-half, was synthesized (Figure 3.1).[6] Irradiation of these molecules at temperatures as low as -80°C, however, did not lead to changes in the UV/vis and CD spectra corresponding to the formation of the expected unstable isomers. In the case of the methoxy-desymmetrized lower-halves, irradiation did lead to *cis*-*trans* isomerization.[7] Therefore, the most probable

explanation for the fact that the formation of the expected unstable isomers was not observed is that the barrier to the thermal helix inversion is reduced to such an extent, that even at very low temperatures the unstable isomers are converted too fast to be analyzed.

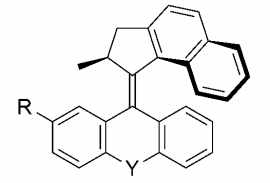

1: Y=O R=H
2: Y=S R=H
3: Y=C(CH_3)$_2$ R=H
4: Y=O R=OMe

Figure 3.1 Second-generation molecular motors **1-4** with a five-membered ring in the upper-half.

3.2.1 Introduction of a Fluorenyl-Based Lower-Half

Because of the fact that the unstable isomer could not be observed experimentally, unidirectionality has not been proven for the photochemical and thermal isomerization behaviour of compounds **1-4**. A direct photoisomerization pathway from stable *cis* to the stable *trans* isomer, and *vise versa*, not involving the anticipated conversion of the unstable isomer to the stable isomer via fast thermal isomerization, cannot be excluded. In order to obtain a second-generation molecular motor with a five-membered ring in the upper-half, anticipated to have faster rates than all previously described light-driven molecular motors, of which unidirectionality of the rotation process could be proven by the observation of the unstable isomer, attempts were made to again increase the isomerization barrier to a small extent. Contraction of the six-membered ring connected to the central double bond in the lower-half of the molecule to a five-membered ring to this end seems counterintuitive at first sight, as this ring-contraction in the upper-half led to a large decrease of the isomerization barrier. The obtained planar fluorenyl-based lower-half, however, is more rigid, leading to different conformational behavior of the fluorenyl-based overcrowded alkene compared to the xanthene-based ones. The second-generation motors containing a fluorenyl-based lower-half appeared to mirror the conformational behavior of bisfluorene in adopting a twisted conformation.[8]

The first examined fluorenyl-based motor **5** employed the phenanthrene-type rotor, connecting an all-carbon six-membered ring to the central alkene, which was used before in the first and second-generation motors. Irradiation of this molecule generated an isomer that appeared to be exceedingly stable compared to all

previous systems, having a half-life at room temperature of about 1300 years! The fact that the upper-half naphthalene moiety has to pass this completely inflexible fluorenyl-based lower-half during the thermal helix inversion probably causes this enormously high energy barrier. Decreasing the size of the upper-half to a five-membered ring in **6** (Figure 3.2) had a huge effect on the energy barrier to the thermal helix inversion: the half-life at room temperature was lowered to 3.2 min![9]

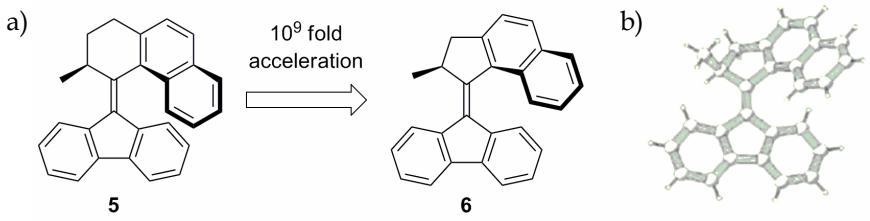

Figure 3.2 a) Acceleration of the thermal isomerization step upon contraction of the six-membered upper-half ring in **5** to a five-membered ring in **6** and b) a Pluto drawing of the X-ray struxture of **6**, showing the complete planarity of the fluorenyl-based lower-half and the overall twisted structure. Reproduced with permission from reference [9]. Copyright 2005 Royal Society of Chemistry.

Since increasing the size of the substituent at the stereocenter had a pronounced effect on the energy barriers of the thermal isomerization steps of the first-generation motors,[10] this strategy was also adopted here. A series of motors possessing substituents of different sizes at the stereocenters was prepared in order to investigate this effect (Table 3.1).[11] In contrast to what was observed for the first-generation motors (see Chapter 2, Scheme 2.1), exchanging the methyl for a slightly more sterically demanding isopropyl group lowered the energy barrier only by a negligible amount. This is consistent with the Winstein-Holness "*A*-values" (the magnitude of the preference of a certain substituent to occupy the equatorial over the axial position of cyclohexane, in $\Delta G°$), that suggest that typically these two substituents have similar steric profiles (A_{Me} = 7.3 kJ, $A_{i\text{-}Pr}$ = 9.2 kJ).[12] Exchanging the methyl group for a phenyl group, which according to its *A*-value (A_{Ph} = 11.7 kJ), and other quantitative measures of steric size, would be expected to also lower the barrier to helix inversion, actually increased the barrier slightly. A possible explanation for this is that the sp^2 hybridization of the phenyl allows it to adopt a conformation parallel to the fluorenyl-based lower-half, minimizing the induced strain. When a *tert*-butyl group was used as the substituent at the stereogenic center in **9**, the most impressive effects were observed. This extra sterically demanding substituent was found to drop the energy barrier to the thermal isomerization by 25 kJ mol^{-1} compared to **6** with a methyl substituent, such that unstable **9** isomerizes 33000 times faster than unstable **6** at room temperature. Its

half-life of 6 milliseconds at room temperature makes it the fastest synthetic unidirectional rotary molecular motor reported so far.[11]

Table 3.1 Effect of the size of the stereogenic substituent on the barrier for thermal helix inversion.

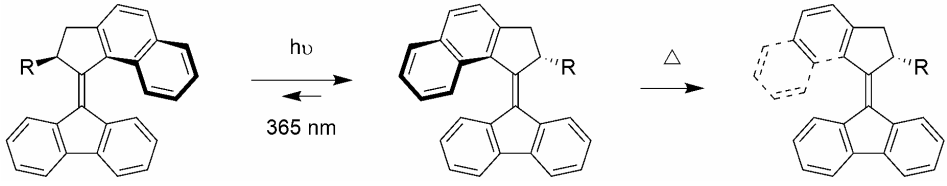

motor	R	*A*-value[12] [kJ]	k° [s^{-1}]	Δ‡*G*° [kJ mol^{-1}]	$t_{½}$ (20°C) [s]
7	Ph	11.7	$1.18 \cdot 10^{-3}$	88	587
6	Me	7.3	$3.64 \cdot 10^{-3}$	85	190
8	*iso*-Pr	9.2	$7.32 \cdot 10^{-3}$	84	95
9	*tert*-Bu	20.1	$1.21 \cdot 10^{2}$	60	$5.74 \cdot 10^{-3}$

3.2.2 Substitution of the Naphthalene for a Substituted Phenyl Moiety

A further redesign of the molecule involved replacement of the naphthalene moieties by substituted phenyl groups.[13] This facilitates the synthesis of functionalized motors, as the need to derivatize the naphthalene moiety through multistep syntheses is avoided. Also another convenient handle for tuning the rotary speed of the motor is generated, as the steric size of the substituent pointing towards the other half of the molecule (into the *fjord* region of the overcrowded alkene), which has to slip past this other half during the thermal isomerization step, can be varied. As a first version of this new design of the light-driven molecular motors, *p*-dimethyl-phenyl-based first-generation motor **10** and second-generation motor **11** were prepared (Figure 3.3). For first-generation motor **10**, the Gibbs energy of activation (Δ‡*G*°) of the unstable *trans* to stable *trans* isomerization amounted 71 kJ mol^{-1}, corresponding to a half-life at room temperature of 1.2 s. This helix inversion is faster than the analogous helix inversion of the related motor containing naphthalene groups, which occurs with a half-life of 18 s under identical conditions. For the unstable *cis* to stable *cis* isomerization, a Gibbs energy of activation of 101.2 kJ mol^{-1} was determined, corresponding to a half-life at room temperature of 1.5 d. This isomerisation step of **10** is much slower than the analogous isomerization of the motor containing naphthalene groups, which has a half-life of 74 min at room temperature. For the thermal isomerization of second-generation motor **11** a Gibbs free energy of activation of 79.1 kJ mol^{-1} was

determined, corresponding to a half-life at room temperature of 15 s. This system rotates 15 times faster than related motor **6** containing naphthalene moieties when irradiated under identical conditions.

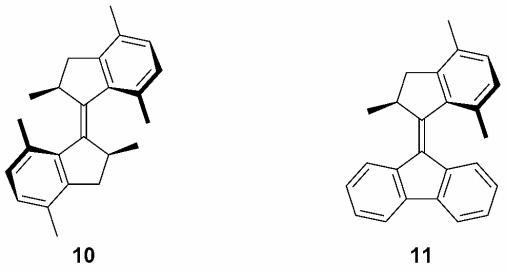

Figure 3.3 Modified first- and second-generation molecular motors **10** and **11**, respectively, in which the naphthalene moieties are replaced by dimethyl substituted phenyl groups.

3.3 New Design for Faster and Functionalizable Molecular Motors

3.3.1 Molecular Design

In order to further elaborate on the effect of structural variations of the substituents on the phenyl ring of newly designed second-generation molecular motor **11**, methoxy-substituted motor **12** was designed (Scheme 3.1).

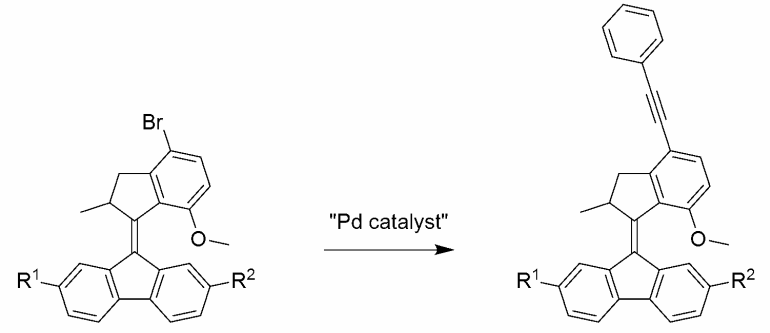

12: R^1, R^2 = H
cis-**13**: R^1 = H, R^2 = OMe
trans-**13**: R^1 = OMe, R^2 = H

14: R^1, R^2 = H
cis-**15**: R^1 = H, R^2 = OMe
trans-**15**: R^1 = OMe, R^2 = H

Scheme 3.1 Newly designed molecular motors **12** and **13**, bearing a bromine functionality which enables further functionalization, for instance via a Sonogashira reaction leading to phenylacetylene-modified motors **14** and **15**.

In this motor molecule, the methyl group that points towards the fluorenyl-based lower-half in **11** is substituted for a methoxy group, which should facilitate the passage of the substituted benzyl moiety along the fluorenyl-based lower-half as the methoxy group is sterically less demanding than the methyl (A_{Me} = 7.7 kJ vs A_{OMe} = 2.7 kJ). This should result in a decreased energy barrier to the thermal helix inversion. Moreover, the introduction of a bromine functionality on the benzyl ring offers the possibility for further functionalization or to link several of these motor molecules to a central scaffold, via palladium catalyzed cross-coupling chemistry such as the Sonogashira reaction. As a proof of this concept, the motors are modified with a phenyl acetylene moiety, leading to motors **14** and **15**, of which the photochemical and thermal isomerizations were analyzed in detail in order to prove that these newly designed systems operate as unidirectional rotary motors.

3.3.2 Synthesis

As discussed in the previous chapter, the key step in the synthesis of these overcrowded alkenes is the coupling of the two halves of the molecule forming the sterically demanding central olefinic bond. Also towards motor molecule **12**, the Staudinger-type diazo-thioketone coupling appeared to be the most suitable synthetic strategy (Scheme 3.2). First, 4-bromoanisole was treated with methacrylic acid in polyphosphoric acid heated to 110°C, giving ketone **18** via a one pot tandem Friedel-Crafts acylation / Nazarov cyclization[14] sequence in a rather poor 24% yield. However, as it is just one step and the first in the synthetic sequence, which can be performed on large scale using commercially available starting materials, it is the preferred route to **18**. Upper-half hydrazone **19** was prepared in 86% by refluxing this ketone in ethanol in the presence of hydrazine monohydrate. The oxidation of hydrazones which, like **19**, contain a fused five-membered ring connected to the hydrazone moiety was shown to be difficult using the standard oxidizing conditions employing Ag_2O. However, hypervalent iodine reagents like [bis(acetoxy)iodo]benzene were shown to be able to oxidize these hydrazones and proved to be a useful alternative method.[6] Thiofluorenone **21**[15] is known to be an unstable compound, and for this reason the next sequence of reactions is needed to be rather precisely timed. First, fluorenone was refluxed in toluene in the presence of Lawesson's reagent for 2½ h. After a quick purification of the thioketone by column chromatography, $PhI(OAc)_2$ was added to a solution of hydrazone **19** in DMF cooled to -50°C, followed directly by the addition of a solution of thioketone **21** in CH_2Cl_2. After the temperature was allowed to reach room temperature over night, the coupling products were isolated as a mixture of episulfide **22** and alkene **12**. Treatment of this mixture with triphenylphosphine in refluxing toluene smoothly converted the episulfide to the desired alkene **12**. The mixture was then treated with methyl iodide in diethyl ether in order to convert the excess triphenylphosphine to the corresponding phosphonium ylide, facilitating the

removal of this compound from the mixture. Alkene **12** was isolated in 40% yield from hydrazone **19**. In the last step, in order to show the amenability of these bromide functionalized motors for further modification, a phenylacetylene moiety was introduced via conditions for the Sonogashira reaction developed by Buchwald, Fu and coworkers.[16] Reaction of **12** with copper iodide, $Pd(PhCN)_2Cl_2$, tri-*tert*-butyl-phosphine and diisopropylamine overnight in dioxane at 50°C gave phenylacetylene-modified motor **14** in 86% yield.

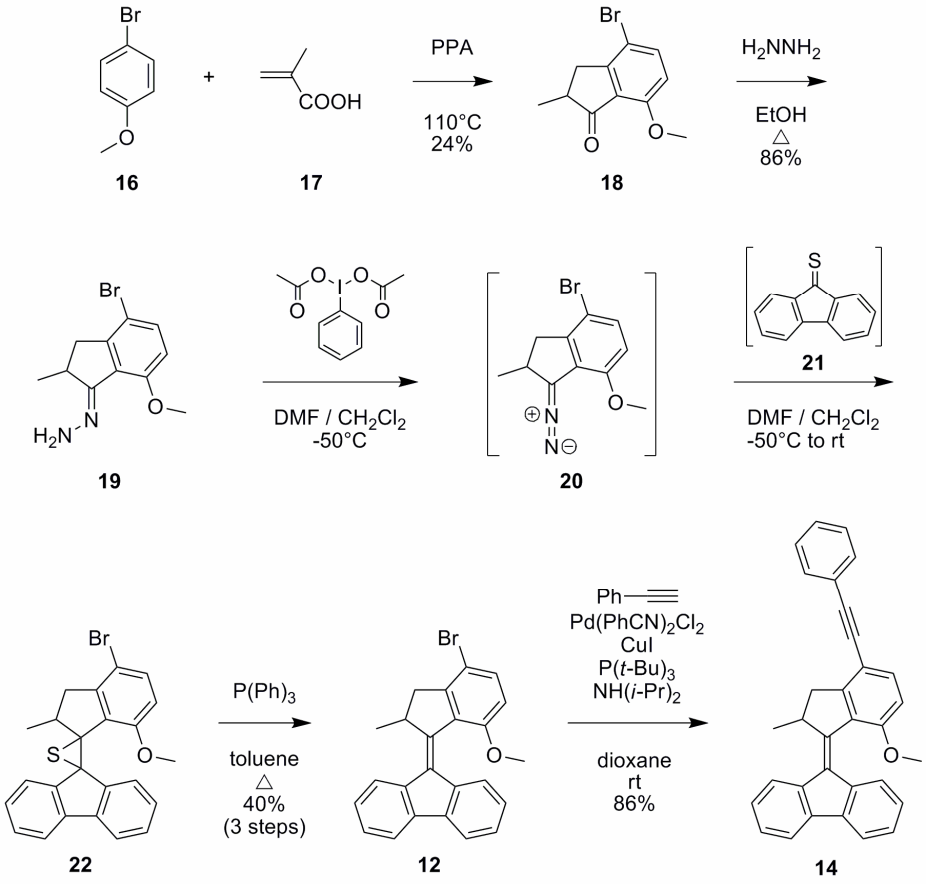

Scheme 3.2 Synthesis of phenylacetylene modified molecular motor **14**, in which a methoxy group occupies the sterically overcrowded region between the two halves of the molecule pointing towards the fluorenyl-based lower-half.

3.3.3 Photochemical and Thermal Isomerization Studies

To validate its operation as a molecular motor, the photochemical and thermal isomerization steps of **14** were studied in detail using low-temperature UV/vis and CD spectroscopy. First, enantioresolution was achieved by HPLC using a chiral stationary phase: separation of (2′*R*)-(*P*)-**14** and (2′*S*)-(*M*)-**14** was feasible on a Chiralcel OD column upon elution with *n*-heptane: isopropanol in a ratio of 95:5. The assignment of the absolute configuration was based on comparison of the CD spectra of the enantiomers with the CD spectra of previously reported second-generation motors.[1] Initially, irradiation (λ = 365 nm) of a sample of (2′*S*)-(*M*)-**14** in *n*-hexane at 20°C did not lead to any changes in both the UV/vis and the CD spectra, suggesting that the thermal isomerization step is fast at room temperature. Cooling of a sample in *iso*-pentane to 150 K appeared to be required to slow down this thermal process sufficiently to allow the detection of (2′*S*)-(*P*)-**14**. Irradiation (λ = 365 nm) of the sample led to a red-shift of the major long-wavelength absorption band in the UV/vis spectrum from around 360 nm to around 400 nm (Figure 3.4a). This red-shift upon the formation of the thermally unstable isomer via the photochemically induced *cis*-*trans* isomerization was also observed for all previously reported fluorenyl-based second-generation molecular motors, where it was attributed to an increase in strain of the central olefinic bond, introduced by the twisted nature of the thermally unstable isomer.[9,11] During irradiation, clear isosbestic points were visible, indicating that the photoisomerization was a clean, unimolecular process. The spectral changes in the UV/vis are accompanied by an inversion of the major absorptions in the CD spectrum (Figure 3.4b), consistent with the inversion of the helicity of the molecule upon the photochemically induced *cis*-*trans* isomerization over the central double bond. The fact that cooling to such low temperatures is required to prevent the thermal process indicates a reduction of the energy barrier to this thermal isomerization by a large extent.

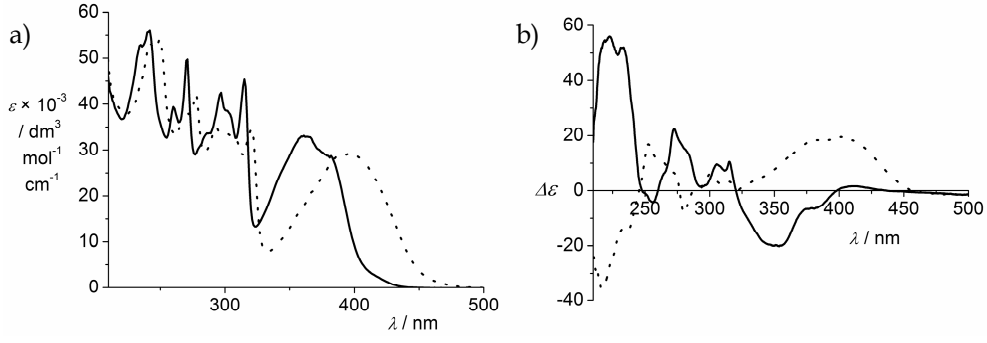

Figure 3.4 UV/vis (a) and CD (b) spectra (*iso*-pentane) of stable (2′*S*)-(*M*)-**14** (solid line), the photostationary state mixture with stable (2′*S*)-(*M*)-**14** and unstable (2′*S*)-(*P*)-**14** (dotted line)

after irradiation (λ = 365 nm, 150 K) (the spectral changes fully reversed after 30 min at 200 K in the dark).

In order to observe the reversal of the spectral changes, corresponding to the conversion of (2′*S*)-(*P*)-**14** to (2′*S*)-(*M*)-**14** via the thermal helix inversion process, "heating" to 200 K was required. The kinetics and thermodynamic parameters of this thermal helix inversion were determined by monitoring the CD absorption at 218 nm over time in the dark at four different temperatures ranging from 167.5 K to 175 K, and subsequently using the various first-order rate constants to calculate the Gibbs energy of activation with the Eyring equation: $\Delta^{\ddagger}G° = 49.1$ kJ mol^{-1} ($\Delta^{\ddagger}H° = 50.7$ kJ mol^{-1}, $\Delta^{\ddagger}S° = 5.5 \pm 0.5$ J mol^{-1} K^{-1}) (see Figure 3.5 for the Eyring plot). By extrapolation of the kinetic data, a half-life of (2′*S*)-(*P*)-**14** at 20 °C of 73 µsec was determined ($k = 9.50 \cdot 10^{3}$ s^{-1}).

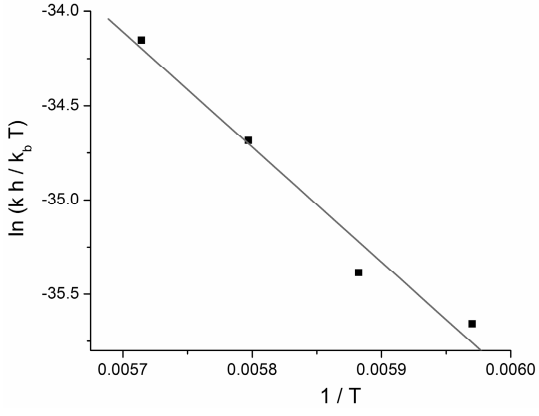

Figure 3.5 Eyring plot for the conversion of (2′*S*)-(*P*)-**14** to (2′*S*)-(*M*)-**14** via the thermal helix inversion.

3.4 Desymmetrization of the Lower-Half

3.4.1 Synthesis

Since **14** contains a symmetric lower-half, just one photochemical and one thermal isomerization step, each accompanied by a helix inversion, convert the olefin to its initial isomer. To be able to identify the four distinct steps that define a full 360° rotary cycle as shown in Scheme 3.4 (*vide infra*), the lower-half of this molecular motor was desymmetized by the introduction of a methoxy substituent. To this end, synthesis of methoxy-desymmetrized thiofluorenone **25** was required (Scheme 3.3).

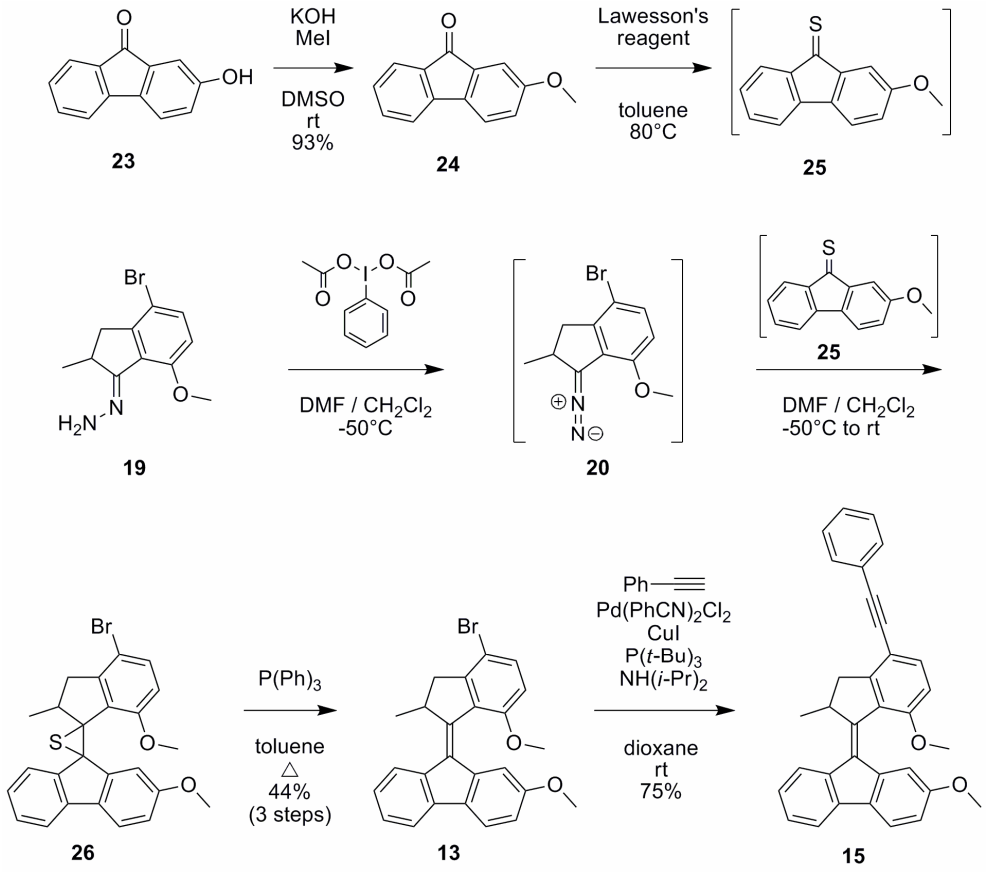

Scheme 3.3 Synthesis of phenylacetylene modified molecular motor **15**, in which a methoxy group occupies the sterically overcrowded *fjord* region between the two halves of the molecule pointing towards the fluorenyl-based lower-half, as well as a methoxy desymmetrized lower-half of the molecule is present.

According to a procedure described by Gualtieri and coworkers,[17] 2-hydroxyfluorenone **23** was treated with potassium hydroxide and methyl iodide, leading to the formation of 2-methoxyfluorenone **24** in 93% yield. This compound was subsequently refluxed in toluene in the presence of Lawesson's reagent, by which it was converted to 2-methoxythiofluorenone **25**. As this compound is rather unstable, it was quickly purified by flash column chromatography and immediately used in the next step. Following exactly the same procedure as was described in the previous section for the synthesis of alkene **14** containing a symmetric lower-half, the coupling reaction starting from upper-half hydrazone **19** and lower-half thioketone **25** was performed. This reaction again produced a

mixture of episulfide **26** and alkene **13**, which was treated with triphenylphosphine to convert the episulfide to desired alkene **13**. The mixture was treated with methyl iodide in diethylether in order to convert the excess triphenylphosphine to the corresponding phosphonium ylide, facilitating the removal of this compound from the mixture. Alkene **13** was obtained in 44% yield from the hydrazone, as a mixture of the *cis* and *trans* isomers, and used as such in the last step. Following a procedure identical to the one described in the previous section for the introduction of the phenylacetylene moiety via Sonogashira conditions towards alkene **14**, alkene **15** was obtained in 75% yield as a mixture of the *cis* and *trans* isomers.

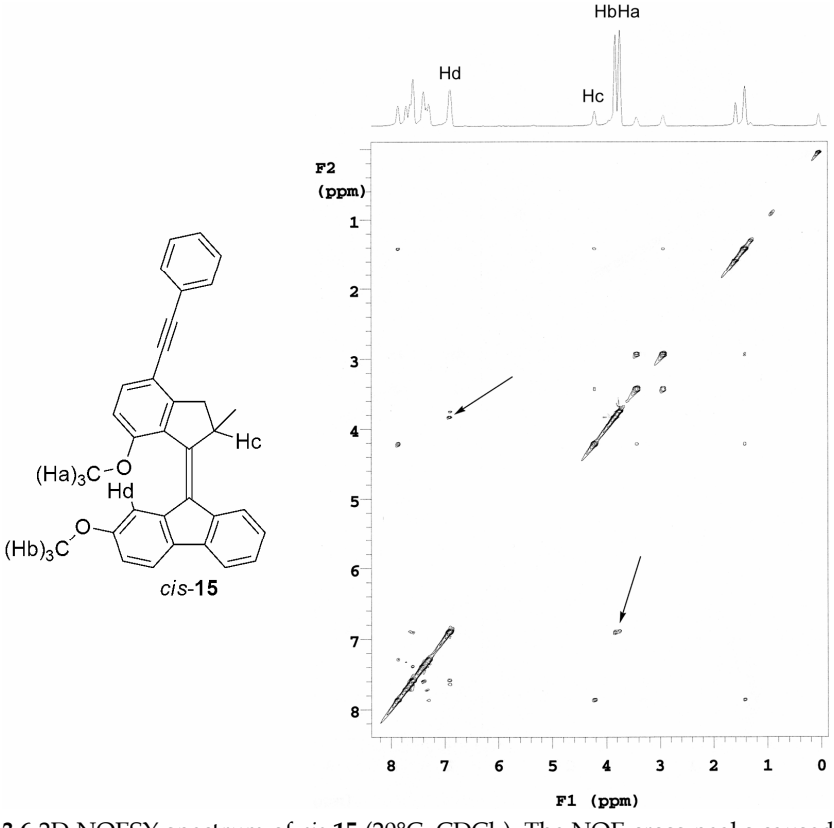

Figure 3.6 2D NOESY spectrum of *cis*-**15** (20°C, $CDCl_3$). The NOE cross peaks caused by the intramolecular interactions are indicated with arrows.

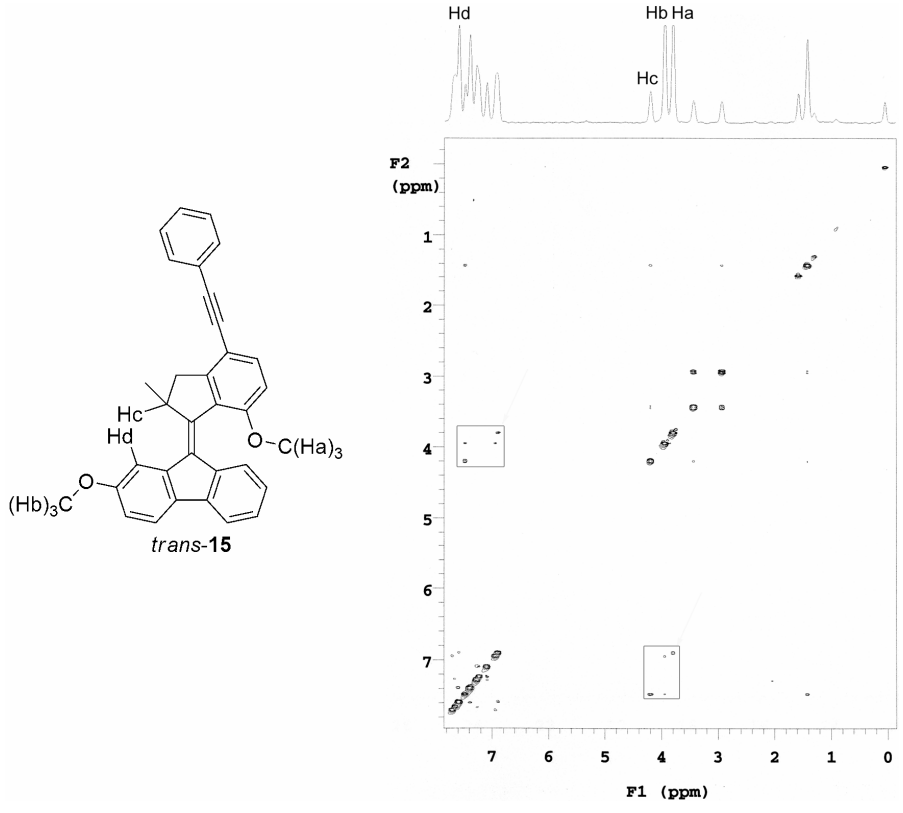

Figure 3.7 2D NOESY spectrum of *trans*-**15** (20°C, $CDCl_3$). The area surrounded by the solid rectangle shows the NOE cross peaks caused by the intramolecular interactions.

3.4.2 Separation and Characterization of the Isomers

Separation of the *cis* and *trans* isomers of alkene **15** containing a methoxy desymmetrized lower-half was achieved by column chromatography over silica using a 12:1 mixture of pentane and *tert*-butyl-methyl ether as the eluent. With the molecular motors containing a naphthalene moiety in the upper-half a strong piece of evidence in assigning the *cis* and *trans* geometrical isomers is provided by the chemical shift of the signal belonging to the methoxy substituent, as shielding of the methoxy protons by the naphthalene moiety in the upper-half of the *cis* isomer causes an upfield shift of this signal of approximately 1 ppm compared to the methoxy signal in the spectrum of the *trans* isomer. The *cis* and *trans* isomers of **15** cannot be unambiguously assigned using the ^{1}H NMR spectra alone, as for both isomers the signals of the two methoxy substituents appear within a spectral region of approximately 0.25 ppm (~3.7-3.9 ppm). Assignment of these geometrical

isomers was therefore pursued by Nuclear Overhauser Enhancement (NOE) spectroscopy.

Indicative for the *cis*-isomer are the cross-couplings between Ha (a singlet at 3.71 ppm) and Hb (a singlet at 3.80 ppm) with Hd (a singlet at 6.82 ppm), and the absence of the cross-coupling between Hc (a multiplet at 4.18 ppm) with Hd (Figure 3.6). Indicative for the *trans*-isomer are the cross-couplings between Hb (a singlet at 3.91 ppm) and Hc (a multiplet at 4.16 ppm) with Hd (a singlet at 7.49 ppm), and the absence of the cross-coupling between Ha (a singlet at 3.76 ppm) with Hd (Figure 3.7).

3.4.3 Photochemical and Thermal Isomerization Studies

With all previously described light-driven molecular motors, unequivocal prove of the unidirectionality of the rotation process performed by these systems was provided by following the photochemical and thermal isomerization processes with ^{1}H NMR. This, however, requires the possibility to irradiate the sample and perform the ^{1}H NMR measurements at sufficiently low temperatures, in order to freeze in the thermal isomerization step and observe and analyze the thermally unstable isomer. For the current system, the NMR tube therefore is required to be kept at 150 K, which made it practically impossible to perform this experiment in our laboratories. Also no deuterated solvents are available, in which the compound is sufficiently soluble, that do not freeze at this temperature. Still several attempts to analyze the photochemical isomerization upon irradiation of a sample of either *cis*-**15** or *trans*-**15** were performed, using as the solvent deuterated Et_2O (mp: -117°C) or mixtures of THF and CH_2Cl_2 that on visual inspection remain liquid (though very viscous) at -115°C, but ^{1}H NMR analysis after 1 h of irradiation at -115°C in all of these cases revealed that no *cis*-*trans* isomerization had taken place. A major problem encountered under the standard conditions employed for this irradiation experiment at these low temperatures is the formation of ice crystals on the NMR tube, blocking the sample from the light source. However, also after irradiation of a sample under Argon atmosphere, preventing the formation of ice crystals, no isomerization was observed by ^{1}H NMR. Recently, the photochemistry of a similar methoxy-substituted second-generation molecular motor was found to be strongly solvent sensitive.[18] Whereas irradiation in apolar *n*-hexane resulted in the expected *cis*-*trans* isomerization, in a polar solvent as CH_2Cl_2 this isomerization was almost completely suppressed. The photochemistry of molecular motor **15** might suffer from this solvent-sensitivity as well, which would explain the failing ^{1}H NMR experiments as these were all performed using polar solvents.

Alternatively, unidirectionality of the rotation process of the current system can also be proven by correlation of the directly determined photostationary state (PSS)

ratios with the ratios of the stable isomers after the thermal helix inversion had taken place. For instance, if the measured PSS ratio of unstable *trans* : stable *cis* of the first photoequilibrium (step 1 in Scheme 3.4) is identical to the ratio of stable *trans* : stable *cis* as measured after heating the sample to room temperature, this proves the unidirectionality of this thermal isomerization which provides unidirectionality of the rotation cycle.

The method that was used to determine the PSS ratios of the two photoequilibria was developed by Fischer[19] and is based on the assumption that the ratio of the quantum yield of the photoconversion of A to B (ϕ_A) over the quantum yield of the photoconversion of B to A (ϕ_B) does not differ at two different wavelengths. As the PSS ratio at any wavelength is a function of these quantum yields and the extinction coefficients according to equation 3.1, this means that the ratio of the two PSS ratios is fully determined by the ratio of the extinction coefficients, or the optical densities (D_A and D_B), at the two wavelengths (equation 3.2).

$$\left(\frac{A}{B}\right)_{\lambda} = \left(\frac{\phi_B}{\phi_A}\right)_{\lambda} \times \left(\frac{\varepsilon_B}{\varepsilon_A}\right)_{\lambda} \qquad \text{(Equation 3.1)}$$

$$\frac{\left(\frac{A}{B}\right)_{\lambda 1}}{\left(\frac{A}{B}\right)_{\lambda 2}} = \frac{\left(\frac{D_B}{D_A}\right)_{\lambda 1}}{\left(\frac{D_B}{D_A}\right)_{\lambda 2}} \qquad \text{(Equation 3.2)}$$

$$\left(\frac{A}{B}\right)_{\lambda} = \left(\frac{1-\alpha}{\alpha}\right)_{\lambda} \qquad \text{(Equation 3.3)}$$

$$\Delta = D_{obs} - D_A \qquad \text{(Equation 3.4)}$$

$$\alpha_{\lambda 2} = \frac{\left(\frac{\Delta_{\lambda 1}}{D_{\lambda 1}} - \frac{\Delta_{\lambda 2}}{D_{\lambda 2}}\right)}{\left(1 + \frac{\Delta_{\lambda 1}}{D_{\lambda 1}} - n\left(1 + \frac{\Delta_{\lambda 2}}{D_{\lambda 2}}\right)\right)} \qquad \text{(Equation 3.5)}$$

By denoting the extent of conversion of A to B by irradiation at any wavelength λ by α (equation 3.3), denoting the change in optical density of the mixture, starting from A to the PSS mixture, by Δ (equation 3.4) and denoting the ratio of the

different PSS ratios obtained by irradiation with two different wavelengths of light by n, equation 3.5 is obtained after developing the expression.

In equation 3.5, the relative amount of B (the thermally unstable isomer) in the PSS ratio of the photoequilibrium after irradiation at the wavelength of interest is expressed as a function of the relative change in absorbance at two particular wavelengths, when passing from pure A (the thermally stable isomer) to the PSS attained by irradiation at the same wavelength, and ratio of the PSS ratios resulting from irradiation by these two wavelengths.

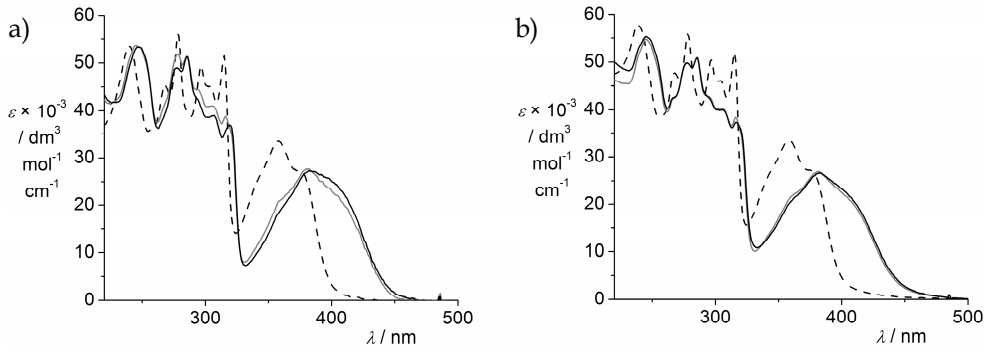

Figure 3.8 UV/vis spectra (*iso*-pentane, 150 K) of (a) stable (2′*S**)-(*M**)-*cis*-**15** (dashed black line), the PSS mixture with stable (2′*S**)-(*M**)-*cis*-**15** and unstable (2′*S**)-(*P**)-*trans*-**15** after irradiation (λ = 365 nm) (solid gray line), the PSS mixture with stable (2′*S**)-(*M**)-*cis*-**15** and unstable (2′*S**)-(*P**)-*trans*-**15** after irradiation (λ = 334 nm) (solid black line) and of (b) stable (2′*S**)-(*M**)-*trans*-**15** (dashed black line), the PSS mixture with stable (2′*S**)-(*M**)-*trans*-**15** and unstable (2′*S**)-(*P**)-*cis*-**15** after irradiation (λ = 365 nm) (solid gray line), the PSS mixture with stable (2′*S**)-(*M**)-*trans*-**15** and unstable (2′*S**)-(*P**)-*cis*-**15** after irradiation (λ = 334 nm) (solid black line).

A sample containing racemic stable (2′*S**)-(*M**)-*cis*-**15**[20] in *iso*-pentane at 150 K was first irradiated with 365 nm light, leading to a red-shift of the long-wavelength band in the UV/vis spectrum from ~360 nm to ~400 nm (Figure 3.8a). Irradiation under identical conditions, however with 334 nm light, led to the same spectral changes, however the long-wavelength band red-shifted slightly further, due to a PSS ratio somewhat more favoring the thermally unstable isomer. The maximal change in optical density (Δ) during both irradiation experiments is observed around 360 nm, and by analysis of the ratio of the Δ's resulting from irradiation at the two different wavelengths at this wavelength, a ratio of the PSS ratios (n) of 1.15 was determined. Furthermore, a relative change in absorbance at 334 nm upon irradiation at this wavelength, $(\Delta/D)_{334}$, of -0.552, and a $(\Delta/D)_{365}$ of -0.305 was determined. From these values, an α of 0.703 can be calculated, which corresponds to a PSS ratio of stable (2′*S**)-(*M**)-*cis*-**15** : unstable (2′*S**)-(*P**)-*trans*-**15** after

irradiation with 365 nm light of 30:70 (step 1 in Scheme 3.4). After allowing the sample to warm to room temperature, the mixture of the stable *cis* and *trans* isomers was analyzed using HPLC, by which an identical ratio of stable (2′*S**)-(*M**)-*cis*-**15** : stable (2′*S**)-(*M**)-*trans*-**15**, of 30:70, was determined. This means that all photochemically induced thermally unstable *trans* isomer, (2′*S**)-(*P**)-*trans*-**15**, is smoothly converted to the corresponding thermally stable *trans* isomer, (2′*S**)-(*M**)-*trans*-**15**, which is a very strong indication for unidirectionality of this thermal isomerization step (step 2 in Scheme 3.4).

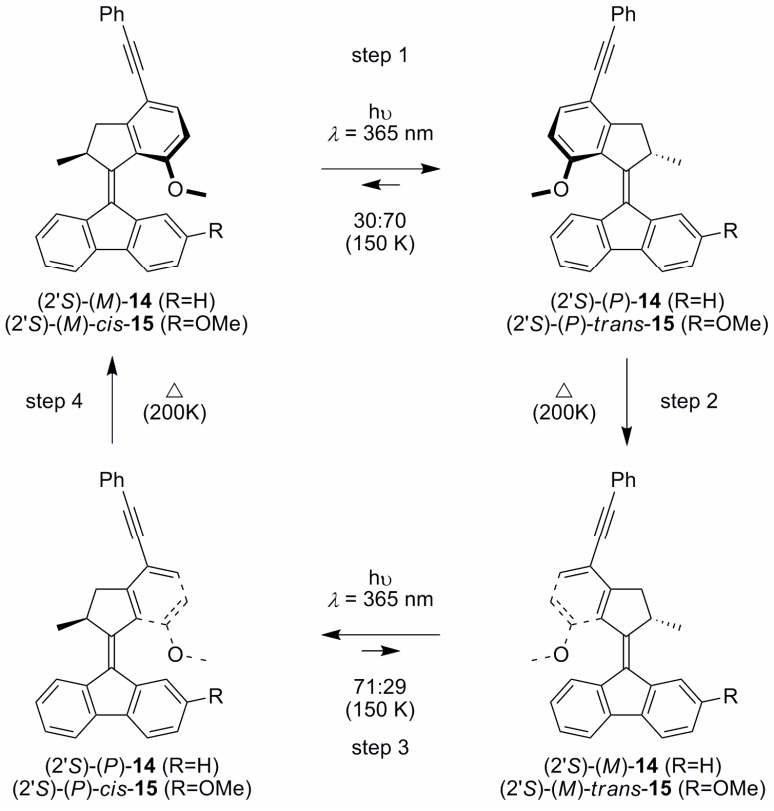

Scheme 3.4 Photochemical and thermal isomerization processes involved with the unidirectional rotary cycle of molecular motor **14** and **15**, containing a symmetric and desymmetrized lower-half, respectively.

Starting from the stable *trans* isomer (Figure 3.8b), no reliable ratio of the PSS ratios (n) could be determined, as the UV/vis spectra at the PSSs after irradiation with the two different wavelengths almost completely overlapped. Therefore, the PSS ratio after irradiation with 365 nm of the second photoequilibrium could not be obtained via the analysis described above. However, comparing the UV/vis

spectra obtained at the PSS of the two photochemical steps (step 1 and 3 in Scheme 3.4, Figure 3.8a vs Figure 3.8b), it has to be concluded that the spectral changes are very similar. Therefore, it can be assumed that also here a photoequilibrium with a PSS ratio of stable (2′*S**)-(*M**)-*trans*-**15** : unstable (2′*S**)-(*P**)-*cis*-**15** after irradiation with 365 nm light of approximately 30:70 is obtained (step 3 in Scheme 3.4). After allowing the sample to warm to room temperature, the mixture of the stable *cis* and *trans* isomers was analyzed using HPLC, by which a ratio of stable (2′*S**)-(*M**)-*trans*-**15** : stable (2′*S**)-(*M**)-*cis*-**15** of 29:71 was determined. This means that all photochemically induced thermally unstable (2′*S**)-(*P**)-*cis*-**15** is smoothly converted to the corresponding stable *cis* isomer, again being a strong indication for unidirectionality of this thermal isomerization step also (step 4 in Scheme 3.4).

Table 3.2 Structural variations within a series of fluorenyl based molecular motor and their effect on the Gibbs energy of activation, rate constant and corresponding half-life at room temperature of the thermal helix inversion step.

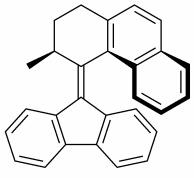

5

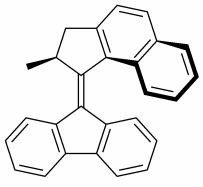

6

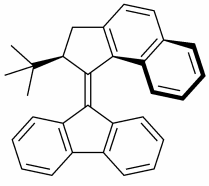

9

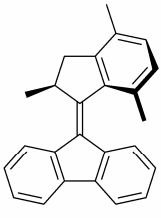

11

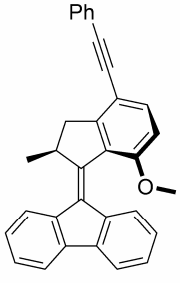

14

motor	$\Delta^{\ddagger}G°$ [kJ mol^{-1}]	k° [s^{-1}]	$t_{½}$ (20°C) [s]
5	139	$1.6 \cdot 10^{-11}$	$>4 \cdot 10^{10}$
6	85	$3.64 \cdot 10^{-3}$	190
9	60	121	$5.74 \cdot 10^{-3}$
11	79	$4.62 \cdot 10^{-2}$	15
14	49	$9.50 \cdot 10^{3}$	$73 \cdot 10^{-6}$

3.5 Discussion and Conclusions

In conclusion, the fluorenyl-based second-generation molecular motors have been shown to be perfectly suitable to tune the rotary speed of, as subtle structural variations have a dramatic influence on the Gibbs energy barrier to the rate determining thermal helix inversion steps (Table 3.2).

Starting from molecule **5**, of which the energy barrier of the thermal step is so high that at room temperature it is practically blocked so that it can effectively be used as a thermally bistable photo-addressable chiroptical switch (a structurally very similar molecule is actually used as such in Chapter 5), eventually molecule **14** is generated, which is capable of operating at 3325 rotations per second,[21] which is 25 times faster than Nature's benchmark molecular motor, F_1-ATPase, which is capable of 130 rotations per second without load at its V_{max}.[3]

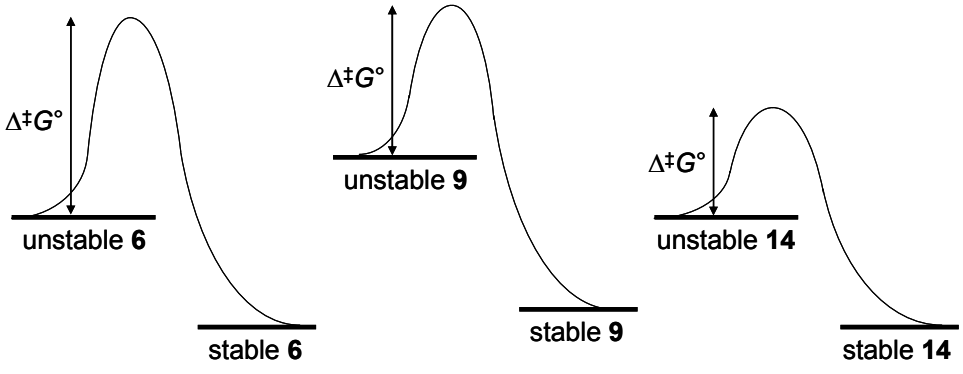

Figure 3.9 Energy profiles for thermal isomerization of **6** (left), **9** (middle) and **14** (right), illustrating the origin of the acceleration by a greater destabilization of the unstable isomer than the stable isomer for **9** and a lowering of the transition state energy for **14**, both resulting in a lower energy barrier.

There is also a marked difference in the way the Gibbs energy barrier to the thermal isomerization is lowered in going from motor **6** to either **9** or **14**. In the first case, the change can be rationalized by considering the Gibbs energy changes experienced by the stable and unstable isomers. The additional steric bulk at the stereocenter results in an increase in strain over the central double bond (the axis of rotation) in the twisted conformation that only the unstable isomer adopts. Therefore the Gibbs energy level of this unstable isomer is raised to a much larger extent by the replacement of the methyl for a *tert*-butyl substituent in going from **6** to **9** compared to the Gibbs energy level of the corresponding stable isomer, which results in the measured drop in Gibbs energy of activation as depicted in Figure

3.9. During the thermal helix inversion of **14**, a sterically less demanding methoxy substituted phenyl moiety passes the lower-half of the molecule instead of a naphthyl group in **6**, which results in a lowered energy barrier, as also shown in Figure 3.9.

Moreover, the presence of the bromide functionality allows for further functionalization of the motor, or coupling of multiple motors to a central scaffold, for instance, via well-established palladium mediated chemistry. As a proof of this concept, a phenylacetylene was introduced in this way, and currently trimer of motors **27** (Figure 3.10), generated by the coupling of multiple motors to a phenyl triacetylene, is under investigation.[22] A large and relatively flat molecule as **27** is amenable to be adsorbed on a surface, where it should be possible to be visualized by scanning probe microscopy techniques. The ultimate aim of this research, currently carried out in our group, would be to induce a movement of the trimer on the surface upon light induced rotation of the motor molecules.

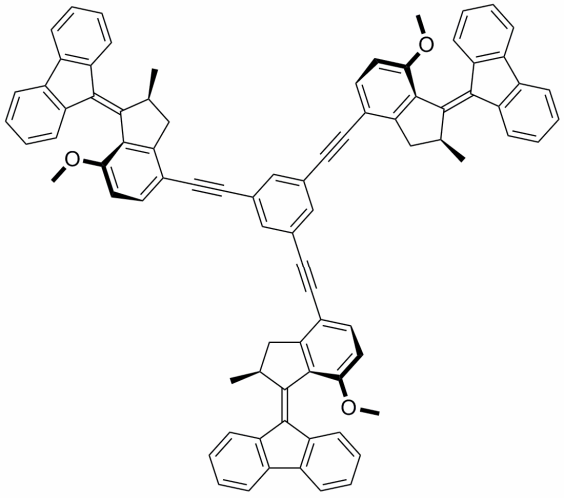

27

Figure 3.10 Molecular motor trimer **27**, designed to lie flat on a surface to be studied by scanning probe microscopy techniques.

Concluding, by structurally redesigning the fluorenyl based molecular motors to system **14**, the fastest artificial light-driven rotary molecular motor developed sofar is obtained, of which the unidirectionality of the rotary behavior could still be demonstrated. Furthermore, its aryl-bromine moiety can be used as a handle to either couple multiple motors to a central scaffold or to introduce other functionalities.

3.6 Acknowledgement

The synthesis of compounds **14** and **15** and several of the spectroscopic studies were performed by Arjen Cnossen during his undergraduate research project (MSc), who is gratefully acknowledged for his contributions.

3.7 Experimental Section

General remarks

For general remarks, see Section 2.6. HPLC analyses and preparative HPLC was performed using a Chiralcel OD (Daicel) column. NOE spectra were recorded on a Varian Unity Plus (500 MHz) spectrometer in $CDCl_3$. Low temperature spectroscopy was established using an OptistatDN (Oxford Instruments, Tubney Woods, Abingdon, Oxon OX13 5QX, UK) cryostat, equipped with a ITC 601 temperature controller. Irradiation experiments were performed with a 200 W Oriel Xe-lamp, adapted with a 300 nm cut-off filter and the appropriate band-pass filter (334 or 365 nm, typical bandwidth: 10 nm) in series, or a Spectroline lamp model ENB-280C/FE (λ = 365 nm).

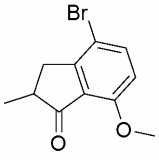

4-Bromo-7-methoxy-2-methyl-2,3-dihydro-1*H*-inden-1-one (18)

To stirred polyphosphoric acid (50 mL) at 65°C was added methacrylic acid **17** (1.50 g, 17.4 mmol). After vigorous stirring for 5 min 4-bromoanisole **16** (3.16 g, 16.9 mmol) was added. The mixture was stirred for 1½ h at 110 °C, whereafter the reaction was quenched by pouring the mixture into 300 mL ice water and stirring the aqueous mixture overnight. The aqueous phase was extracted with 2 x 150 mL Et_2O. The combined organic layers were filtered, washed with water and brine, and dried over Na_2SO_4. After removal of the solvent *in vacuo* the crude product was further purified by column chromatography (SiO_2, *n*-heptane:EtOAc = 2:1) yielded **18** (1.02 g, 24%) as a light yellow oil which solidified on standing. ^{1}H NMR (400 MHz, $CDCl_3$) δ 1.21 (d, *J* = 7.6 Hz, 3H), 2.49 (dd, *J* = 17.6, 4.4 Hz, 1H), 2.58-2.62 (m, 1H), 3.18 (dd, *J* = 17.6, 8.0 Hz, 1H), 3.85 (s, 3H), 6.64 (d, *J* = 8.8 Hz, 1H), 7.54 (d, *J* = 8.8 Hz, 1H); ^{13}C NMR (50 MHz, $CDCl_3$) δ 16.7 (q), 36.0 (t), 42.2 (d), 56.2 (q), 111.5 (d), 111.9 (s), 126.3 (s), 138.8 (d), 155.2 (s), 157.6 (s), 206.5 (s); *m/z* (EI^+, %) = 254 (M^+, 100), 225 (92); HRMS (EI^+): calcd for $C_{11}H_{11}O_2Br$ 253.9942, found 253.9930.

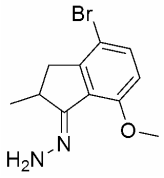

(4-Bromo-7-methoxy-2-methyl-2,3-dihydro-1*H*-inden-1-ylidene)hydrazine (19)

Ketone **18** (0.887 g, 3.47 mmol) was dissolved in hydrazine monohydrate (20 mL) and heated to reflux for 1 h, during which a precipitate was formed. The reaction mixture was allowed to cool and the light yellow precipitate was filtered off and washed twice with cold ether. The mother liquor was taken up in EtOAc and washed with water. Drying over Na_2SO_4 and removal of the solvent yielded a second portion of **19** as a light brown solid (combined yield 0.80 g, 86%). mp 152-154°C; ^{1}H NMR (400 MHz, $CDCl_3$) δ 1.23 (d, *J* = 7.2 Hz, 3H), 2.56 (d, *J* = 16.8 Hz, 1H), 3.17-3.27 (m, 2H), 3.89 (s, 3H), 5.35 (b, 2H), 6.67 (d, *J* = 8.8 Hz, 1H), 7.33 (d, *J* = 8.8 Hz, 1H); ^{13}C NMR (75 MHz, $CDCl_3$) δ 17.3 (q), 32.2 (d), 39.9 (t), 56.3 (q), 111.5 (d), 111.7 (s), 126.7 (s), 132.7 (d), 147.2 (s), 155.8 (s), 160.0 (s); *m/z* (EI^+, %) = 268 (M^+, 86), 252 (100); HRMS (EI^+): calcd for $C_{11}H_{11}NOBr$ [M-NH_2] 252.0024, found 252.0017; Anal. calcd for $C_{11}H_{13}N_2OBr$: C, 49.09; H, 4.87; N, 10.41, found: C, 48.86 H, 4.84; N, 10.31.

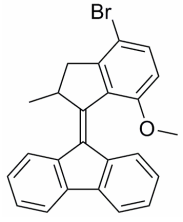

9-(4-Bromo-7-methoxy-2-methyl-2,3-dihydro-1*H*-inden-1-ylidene)-9*H*-fluorene (12)

To a solution of 9-fluorenone (0.351 g, 1.95 mmol) in toluene (5 mL) was added Lawesson's reagent (1.17 g, 2.89 mmol). The mixture was heated to reflux for 2½ h. The toluene was distilled *in vacuo* and the residue purified by column chromatography (SiO_2, *n*-pentane:CH_2Cl_2 = 1:1, R_f = 0.8) yielding thioketone **21** as a green solid (0.200 g, 52%). To a solution of hydrazone **19** (0.204 g, 0.76 mmol) in DMF (5 mL), stirred at -50°C, was added [bis(acetoxy)iodo]benzene (0.29 g, 0.91 mmol) followed, after 20 sec of stirring, by a solution of thioketone **21** (0.200 g, 1.02 mmol) in CH_2Cl_2 (5 mL). The mixture was allowed to warm to room temperature overnight and diluted with EtOAc. The organic layer was washed with water, 2N aqueous HCl and brine and concentrated. Column chromatography (SiO_2, *n*-pentane:CH_2Cl_2 = 9:1) yielded 0.14 g of a yellow solid, which by ^{1}H NMR was

identified as a mixture of episulfide **22** (R_f = 0.4) and alkene **12** (R_f = 0.35). Episulfide **22**: ^{1}H NMR (400 MHz, $CDCl_3$) δ 1.25 (d, *J* = 6.9 Hz, 3H), 2.35 (d, *J* = 15.8 Hz, 1H), 2.47 (dd, *J* = 15.8, 5.9 Hz, 1H), 2.96-3.00 (m, 1H), 3.94 (s, 3H), 6.68 (d, *J* = 8.8 Hz, 1H), 7.08 (t, *J* = 7.8 Hz, 1H), 7.22-7.45 (m, 5H), 7.65 (d, *J* = 7.6 Hz, 1H), 7.72 (d, *J* = 7.8 Hz, 2H); *m/z* (EI^+, %) = 434 (M^+, 42), 308 (100). This mixture was dissolved in toluene (10 mL) and triphenylphosphine (0.78 g, 3 mmol) was added. The solution was refluxed 20 h and the toluene was distilled *in vacuo*. The residue was taken up in Et_2O (12 mL) and MeI (1 mL) was added. The reaction mixture was stirred for 3 h, upon which a white precipitate formed. This precipitate was filtered off and the filtrate was concentrated. Column chromatography (SiO_2, *n*-pentane:CH_2Cl_2 = 9:1, R_f = 0.45) yielded alkene **12** (0.123 g, 40%) as a yellow solid. mp 149-150°C; ^{1}H NMR (300 MHz, $CDCl_3$) δ 1.41 (d, *J* = 6.7 Hz, 3H), 2.75 (d, *J* = 15.6 Hz, 1H), 3.32 (dd, *J* = 15.5, 5.9 Hz, 1H), 3.72 (s, 3H), 4.16-4.20 (m, 1H), 6.76 (d, *J* = 8.7 Hz, 1H), 7.17 (t, *J* = 8.0 Hz, 1H), 7.25-7.40 (m, 5H), 7.76 (d, *J* = 7.5 Hz, 1H), 7.78-7.81 (m, 1H), 7.87-7.89 (m, 1H); ^{13}C NMR (50 MHz, $CDCl_3$) δ 19.5 (q), 42.8 (t), 43.6 (d), 55.2 (q), 111.7 (d), 111.9 (s), 119.1 (d), 120.0 (d), 124.5 (d), 125.6 (d), 126.2 (d), 127.3 (d), 127.4 (d), 127.5 (d), 130.9 (s), 131.8 (s), 133.5 (d), 138.1 (s), 139.7 (s), 139.8 (s), 140.5 (s), 147.4 (s), 148.9 (s), 156.5 (s); *m/z* (EI^+, %) = 402 (M^+, 91), 308 (100); HRMS (EI^+): calcd for $C_{24}H_{19}OBr$ 402.0617, found 402.0619.

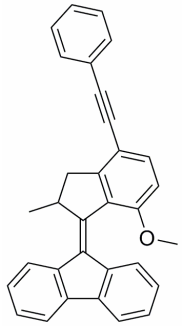

9-(7-Methoxy-2-methyl-4-(phenylethynyl)-2,3-dihydro-1*H*-inden-1-ylidene)-9*H*-fluorene (14)

Following the general procedure for the Sonogashira reaction described by Buchwald, Fu and coworkers,[16] in a flame-dried flask under N_2 was placed CuI (0.7 mg, 3.6 µmol), $Pd(PhCN)_2Cl_2$ (2.1 mg, 5.4 µmol), P(*t*-Bu)$_3$ (2.2 mg, 10.8 µmol), diisopropylamine (24 µL, 18 mg, 0.18 mmol), alkene **12** (39 mg, 0.09 mmol), phenylacetylene (12 µL, 11 mg, 0.11 mmol) and dioxane (0.3 mL). The reaction mixture was stirred overnight at room temperature and diluted with EtOAc. The organic layer was washed with water, 2N aqueous HCl and brine. The solvent was removed *in vacuo* and the crude product was further purified by column chromatography (SiO_2, *n*-pentane:CH_2Cl_2 = 6:1, R_f = 0.6) to yield alkene **12** as a

yellow solid (33 mg, 86%). ^{1}H NMR (400 MHz, $CDCl_3$) δ 1.40 (d, *J* = 6.7 Hz, 3H), 2.92 (d, *J* = 15.6 Hz, 1H), 3.42 (dd, *J* = 15.6, 6.0 Hz, 1H), 3.76 (s, 3H), 4.18-4.22 (m, 1H), 6.87 (d, *J* = 8.4 Hz, 1H), 7.15 (t, *J* = 8.2 Hz, 1H), 7.25-7.40 (m, 7H), 7.54-7.59 (m, 3H), 7.74 (d, *J* = 7.6 Hz, 1H), 7.78-7.81 (m, 1H), 7.88-7.91 (m, 1H); ^{13}C NMR (100 MHz, $CDCl_3$) δ 19.1 (q), 40.9 (t), 43.7 (d), 54.8 (q), 87.3 (s), 91.4 (s), 109.6 (d), 113.1 (s), 118.6 (d), 119.6 (d), 123.5 (s), 124.1 (d), 125.2 (d), 125.8 (d), 126.8 (d), 126.9 (d), 128.1 (d), 128.3 (2×d), 128.9 (s), 130.8 (s), 131.5 (2×d), 133.8 (d), 137.9 (s), 139.4 (s), 139.5 (s), 140.1 (s), 147.3 (s), 151.9 (s), 156.9 (s); *m/z* (EI$^+$, %) = 424 (M$^+$, 100), 409 (81); HRMS (EI$^+$): calcd for $C_{32}H_{24}O$ 424.1827, found 424.1825.

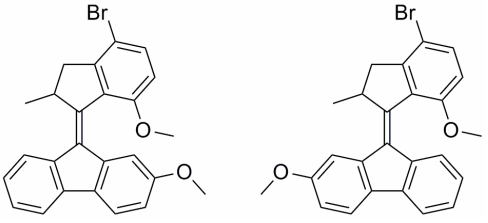

(*E*)/(*Z*)-9-(4-Bromo-7-methoxy-2-methyl-2,3-dihydro-1*H*-inden-1-ylidene)-2-methoxy-9*H*-fluorene (13)

To a solution of 2-methoxy-9H-fluoren-9-one **24**[17] (0.138 g, 0.66 mmol) in toluene (3 mL) was added Lawesson's reagent (0.405 g, 1 mmol). The mixture was heated to 80°C for 3 h. The toluene was removed by distillation *in vacuo* and the residue purified by column chromatography (SiO_2, *n*-pentane:CH_2Cl_2 = 1:1, R_f = 0.8). The first (wine-red colored) band, containing thioketone **25**, was collected, concentrated and then immediately used in the next step. To a solution of hydrazone **19** (53 mg, 0.2 mmol) in DMF (2 mL), stirred at -50°C, was added [bis(acetoxy)iodo]benzene (76 mg, 0.24 mmol) followed, after 20 sec of stirring, by a solution of thioketone **25** in CH_2Cl_2 (2 mL). The mixture was allowed to warm to room temperature overnight and diluted with EtOAc. The organic layer was washed with water, 2 N aqueous HCl and brine and dried on Na_2SO_4. The solvent was removed *in vacuo* and the crude product was purified by column chromatography (SiO_2, *n*-pentane:CH_2Cl_2, gradient 4:1 to 2:1) yielding a mixture of episulfide **26** (R_f = 0.3) and alkene **13** (R_f = 0.25) in a combined yield of 45 mg. This mixture was dissolved in toluene (8 mL) and triphenylphosphine (0.24 g, 0.92 mmol) was added. The solution was refluxed overnight, after which the toluene was removed by distillation *in vacuo*. The residue was taken up in Et_2O (12 mL) and MeI (1 mL) was added. The reaction mixture was stirred for 3 h, upon which a white precipitate formed. This precipitate was filtered off and the filtrate was concentrated. Column chromatography (SiO_2, *n*-pentane:CH_2Cl_2 = 2:1, R_f = 0.6) yielded alkene **13** (38 mg, 44% from hydrazone **19**) as a yellow solid, and as a mixture of the *cis* and *trans* isomers. ^{1}H NMR (300 MHz, $CDCl_3$) δ 1.36-1.39 (m, 6H), 2.72 (d, *J* = 14.4, 2H), 3.28

(dd, *J* = 15.1, 6.0 Hz, 2H), 3.72 (s, 6H), 3.75 (s, 3H), 3.91 (s, 3H), 4.17-4.21 (m, 2H), 6.84-6.94 (m, 6H), 7.06 (t, *J* = 7.4 Hz, 1H), 7.18-7.40 (m, 9H), 7.44 (s, 1H), 7.53-7.70 (m, 10H), 7.84 (d, *J* = 7.7 Hz, 1H); ^{13}C NMR (75 MHz, $CDCl_3$) δ 18.9 (q), 19.1 (q), 42.4 (2×t), 43.2 (d), 43.3 (d), 54.9 (q), 55.1 (q), 55.4 (q), 55.6 (q), 110.7 (d), 111.1 (d), 111.3 (d), 111.4 (s+d), 111.5 (s), 112.4 (d), 113.0 (d), 118.0 (d), 118.9 (d), 119.2 (d), 120.1 (d), 124.1 (d), 124.8 (d), 125.0 (d), 125.8 (d), 127.1 (d), 127.2 (d), 130.5 (s), 131.5 (s), 132.9 (s), 133.1 (d), 133.2 (d), 133.6 (s), 137.6 (s), 139.2 (s), 139.3 (s), 139.5 (s), 140.2 (s), 140.9 (s), 147.0 (s), 148.4 (2×s), 148.5 (2×s), 156.1 (2×s), 158.8 (2×s), 159.3 (s); *m/z* (EI^+, %) = 434 (M^+, 100), 338 (93); HRMS (EI^+): calcd for $C_{25}H_{21}O_2Br$ 434.0705, found 434.0700.

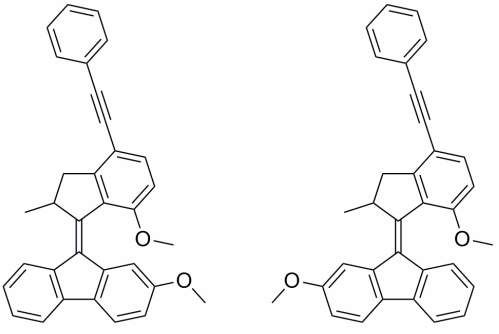

(*E*)/(*Z*)-9-(7-Methoxy-2-methyl-4-(phenylethynyl)-2,3-dihydro-1*H*-inden-1-ylidene)-2-methoxy-9*H*-fluorene (15)

Following the general procedure for the Sonogashira reaction described by Buchwald, Fu and coworkers,[16] in a flame-dried flask under N_2 was placed CuI (0.5 mg, 2.6 µmol), $Pd(PhCN)_2Cl_2$ (1.6 mg, 4.1 µmol), P(*t*-Bu)$_3$ (2.0 µL, 2.2 mg, 8.3 µmol), diisopropylamine (19 µL, 14 mg, 0.14 mmol), alkene **13** (19 mg, 0.044 mmol), phenylacetylene (9.1 µL, 8.5 mg, 0.083 mmol) and 1,4-dioxane (0.25 mL). The solution was stirred overnight at 50°C and then diluted with EtOAc. The organic layer was washed with water, 2 N aqueous HCl and brine, and dried on Na_2SO_4. The solvent was removed *in vacuo* and the crude product was further purified by column chromatography (SiO_2, *n*-pentane:CH_2Cl_2 = 3:1, R_f = 0.7) to yield alkene **15** as a yellow solid (15 mg, 75%) as a mixture of the *cis* and *trans* isomers. The *cis* and *trans* isomers were subsequently separated by column chromatography (SiO_2, *n*-pentane:*t*-BuOMe = 12:1). *Cis*-**15** (R_f = 0.35): ^{1}H NMR (400 MHz, $CDCl_3$) δ 1.38 (d, *J* = 6.7 Hz, 3H), 2.90 (d, *J* = 15.5 Hz, 1H), 3.40 (dd, *J* = 15.5, 5.9 Hz, 1H), 3.71 (s, 3H), 3.80 (s, 3H), 4.16-4.20 (m, 1H), 6.84-6.89 (m, 3H), 7.25-7.40 (m, 5H), 7.53-7.57 (m, 3H), 7.61 (d, *J* = 7.9 Hz, 1H), 7.68 (d, *J* = 7.4 Hz, 1H), 7.83 (d, *J* = 7.3 Hz, 1H); ^{13}C NMR (125 MHz, $CDCl_3$) δ 19.1 (q), 40.8 (t), 43.8 (d), 55.0 (q), 55.4 (q), 87.2 (s), 91.4 (s), 109.7 (d), 111.0 (d), 113.0 (d), 113.2 (d), 118.9 (d), 119.2 (d), 123.6 (s), 124.1 (d), 125.8 (d), 127.1 (d), 128.1 (d), 128.4 (2×d), 128.9 (s), 131.0 (s), 131.6 (2×d), 133.0 (s),

134.0 (d), 139.5 (s), 139.6 (s), 140.2 (s), 147.4 (s), 152.1 (s), 157.0 (s), 158.9 (s). *Trans*-**15** (R_f = 0.25): ^{1}H NMR (200 MHz, $CDCl_3$) δ 1.39 (d, *J* = 6.8 Hz, 3H), 2.90 (d, *J* = 15.4 Hz, 1H), 3.41 (dd, *J* = 15.8, 5.6 Hz, 1H), 3.76 (s, 3H), 3.91 (s, 3H), 4.16-4.20 (m, 1H), 6.88 (t, *J* = 8.0 Hz, 2H), 7.05 (t, *J* = 7.2 Hz, 1H), 7.15-7.60 (m, 10H), 7.66 (d, *J* = 8.0 Hz, 1H); ^{13}C NMR (125 MHz, $CDCl_3$) δ 18.9 (q), 40.9 (t), 43.7 (d), 54.8 (q), 55.6 (q), 55.6 (q), 87.2 (s), 91.4 (s), 109.7 (d), 110.7 (d), 112.3 (d), 113.1 (s), 117.9 (d), 120.1 (d), 123.5 (s), 124.7 (d), 125.0 (d), 126.9 (d), 128.1 (d), 128.3 (2×d), 128.9 (d), 130.8 (d), 131.5 (2×d), 133.5 (s), 133.8 (d), 137.8 (s), 139.4 (s), 141.0 (s), 147.3 (s), 151.9 (s), 156.9 (s), 159.2 (s); *m/z* (EI^+, %) = 454 (M^+, 100), 439 (80); HRMS (EI^+): calcd for $C_{33}H_{26}O_2$ 454.1933, found 454.1921.

3.8 References

[1] a) N. Koumura, E. M. Geertsema, A. Meetsma, B. L. Feringa, *J. Am. Chem. Soc.* **2000**, *122*, 12005-12006; b) N. Koumura, E. M. Geertsema, M. B. van Gelder, A. Meetsma, B. L. Feringa, *J. Am. Chem. Soc.* **2002**, *124*, 5037-5051.

[2] D. Pijper, R. A. van Delden, A. Meetsma, B. L. Feringa, *J. Am. Chem. Soc.* **2005**, *127*, 17612-17613.

[3] a) K. Kinosita, K. Adachi, H. Itoh, *Annu. Rev. Biophys. Biomol. Struct.* **2004**, *33*, 245-268; b) H. Noji, *F1-Motor of ATP Synthase*, Ch. 5 in *Molecular Motors* (Ed.: M. Schliwa), Wiley-VCH, Weinheim, **2003**; c) M. G. L. van den Heuvel, C. Dekker, *Science* **2007**, *317*, 333-336.

[4] For a recent review on the tuning of the speed of these molecular motors, see: M. M. Pollard, M. Klok, D. Pijper, B. L. Feringa, *Adv. Funct. Mater.* **2007**, *17*, 718-729.

[5] M. K. J. ter Wiel, R. A. van Delden, A. Meetsma, B. L. Feringa, *J. Am. Chem. Soc.* **2003**, *125*, 15076-15086.

[6] M. K. J. ter Wiel, J. Vicario, S. G. Davey, A. Meetsma, B. L. Feringa, *Org. Biomol. Chem.* **2005**, *3*, 28-30.

[7] M. K. J. ter Wiel, Ph.D. Thesis, University of Groningen, **2004**, Ch. 4.

[8] P. U. Biedermann, J. J. Stezowski, I. Agranat, *Eur. J. Org. Chem.* **2001**, 15-34.

[9] J. Vicario, A. Meetsma, B. L. Feringa, *Chem. Commun.* **2005**, 5910-5912.

[10] M. K. J. ter Wiel, R. A. van Delden, A. Meetsma, B. L. Feringa, *J. Am. Chem. Soc.* **2005**, *127*, 14208-14222.

[11] J. Vicario, M. Walko, A. Meetsma, B. L. Feringa, *J. Am. Chem. Soc.* **2006**, *128*, 5127-5135.

[12] E. V. Ansyln, D. A. Dougherty, *Modern Physical Organic Chemistry*, 1st ed., University Science Books, Sausalito, **2005**, Ch. 2. The steric size of a substituent is, however, always context-dependent; for an overview of alternative qualitative measures of steric size, see: H. Förster, F. Vögtle, *Angew. Chem., Int. Ed.* **1977**, *16*, 429-441.

[13] M. M. Pollard, A. Meetsma, B. L. Feringa, *Org. Biomol. Chem.* **2008**, 507-512.

[14] For this reaction on dimethylbenzene, see: W. Kaminsky, O. Rabe, A.-M. Schauwienold, G. U. Schupfner, J. Hanss and J. Kopf, *J. Organomet. Chem.* **1995**, *497*, 181-193.

[15] S. Scheibye, R. Shabana, S.-O. Lawesson, C. Rømming, *Tetrahedron* **1982**, *38*, 993-1001.

[16] T. Hundertmark, A. F. Littke, S. L. Buchwald, G. C. Fu, *Org. Lett.* **2000**, *2*, 1729-1731.

[17] S. Dei, E. Teodori, A. Garnier-Suillerot, F. Gualtieri, S. Scapecchi, R. Budriesi, A. Chiarini, *Bioorg. Med. Chem.* **2001**, *9*, 2673-2682.
[18] M. M. Pollard, P. Wesenhagen, D. Pijper, B. L. Feringa, *Org. Biomol. Chem.*, accepted.
[19] E. Fischer, *J. Phys. Chem.* **1967**, *71*, 3704-3706.
[20] The asterisks indicate the fact that a racemic mixture of (2'*S*)-(*M*)-*cis*-**15** and (2'*R*)-(*P*)-*cis*-**15** was used, the absolute configuration and helicity of one of the enantiomers is given here for clarity.
[21] This number is based on the rate of the thermal step ($k = 9500\ s^{-1}$), in combination with the position of the photoequilibrium (30:70 in favor of the unstable isomer, by irradiation with an appropriate light source), divided by 2 (as two thermal conversions are needed to fulfill a complete rotation): (9500 * 0.7)/2.
[22] A. Cnossen, D. Pijper, T. Kudernáč, M. M. Pollard, B. L. Feringa, manuscript in preparation.